

# EFFECT OF MELT STRUCTURE ON EVAPORATION COEFFICIENTS AND ISOTOPIC FRACTIONATION FACTORS. R. A. Mendybaev<sup>1</sup>, B. A. Kowalski<sup>2</sup>, P. S. Savage<sup>3</sup> and N. S. Jacobson<sup>2</sup>.

<sup>1</sup>Department Geophys. Sci., University of Chicago, Chicago, IL 60637 ([ramendyb@uchicago.edu](mailto:ramendyb@uchicago.edu)); <sup>2</sup>NASA Glenn Research Center, Cleveland, OH 44135; <sup>3</sup>School Earth Environment. Sci., St. Andrews, KY16 9TS.

**Introduction:** Coarse-grained igneous textures of Type B and Compact Type A CAIs suggest their formation by slow cooling (<50°C/hr) of at least partially molten droplets [1, 2]. If melting occurs under low-pressure conditions, the evaporative loss of moderately volatile elements (e.g., Mg, Si) would result in large chemical and mass-dependent isotopic fractionations. These features have been reproduced in laboratory experiments in which CAI-like melts have been evaporated in vacuum and low pressure H<sub>2</sub> gas ([3] and references therein).

The next logical step is to develop an accurate model of evaporation to quantitatively describe the chemical and isotopic evolution of *any* CAI-like melt. Chemical evolution of such a melt can be modeled by calculating evaporative flux  $J_i$  of an element  $i$  using Hertz-Knudsen equation  $J_i = \gamma_i P_{i,sat} / \sqrt{2\pi m_i RT}$ . This approach requires knowledge of: 1) equilibrium vapor pressures  $P_{i,sat}$  of species above the melt (or activities of oxides  $a_i$  in the melt), and 2) evaporation coefficient  $\gamma_i$  of an element  $i$  evaporating from the melt.  $P_{i,sat}$  and  $a_i$  can be calculated using an appropriate thermodynamic model for CMAS melt. Evaporation coefficient, which is the kinetic parameter that defines effectiveness of evaporation of a component  $i$  from the surface of solids or liquids in an open system, can only be determined experimentally by measuring free-surface and equilibrium evaporation fluxes:  $\gamma_i = J_{i,free} / J_{i,eq}$ . Since  $\gamma_i$ s vary from ~1 to 10<sup>-6</sup> even for simple oxides, knowledge of  $\gamma_i$  becomes critically important to model chemical evolution of evaporating melt.

Isotopic evolution of evaporating melt can be modeled using the relationship  $R_{2,1} = R_0 f_i^{\alpha_{2,1}-1}$  ( $R_{2,1}$  and  $R_0$  are the ratio of isotopes 2 and 1 of  $i$  in the evaporation residue and in the starting material,  $f_i$  is the fraction of isotope 1 remaining in the residue) if isotopic fractionation factors  $\alpha_i$ s are known. Although  $\alpha_i$ s have been determined for a number of melilitic and forsteritic CAI-like melts the effect of melt structure on  $\alpha_i$ s is still not clear. For example, no such data exist for anorthitic or pyroxene composition melts.

To eliminate possible effect of magnesium on evaporation of silicon from CMAS system we first concentrate on CaO-Al<sub>2</sub>O<sub>3</sub>-SiO<sub>2</sub> system. Here we report experimental results on free and equilibrium evaporation of SiO<sub>2</sub> and CaAlSi<sub>2</sub>O<sub>8</sub> (AN) melts that were then used to determine evaporation coefficient of silicon and its isotopic fractionation factor.

**Experimental:** The experiments were conducted

at the University of Chicago using high-T vacuum furnace (see [3] for details) and vacuum TGA [4] at NASA Glenn Research Center. In free evaporation experiments we used premolten samples loaded into 2.5 mm dia Ir-wire loops, while the Ir-cell with 1.0 mm orifice was used in the equilibrium experiments. Iridium was chosen as a cell material because it is refractory and chemically inert element with respect to silica and silicate melts.

Since the effective temperature of the transparent molten SiO<sub>2</sub> is significantly lower than the effective furnace temperature [5], as a starting material in the SiO<sub>2</sub> experiments we used SiO<sub>2</sub> powder mixed with 1 wt % of ultrafine metallic iridium. AN melt (43.2 wt% SiO<sub>2</sub>, 20.2% CaO, 36.7% Al<sub>2</sub>O<sub>3</sub>) was prepared by mixing appropriate amounts of high-purity SiO<sub>2</sub>, CaCO<sub>3</sub> and Al<sub>2</sub>O<sub>3</sub> powders. Evaporation residues from the experiments with fixed duration (up to 3 hr) were used for chemical and isotopic composition studies. Chemical composition of the evaporation residues was obtained using the TESCAN LYRA3 FIB/FESEM at the University of Chicago. The silicon isotopic composition of the evaporation residues was measured at the University of St Andrews using method described in [6].

## Results and Discussion:

1) *Evaporation kinetics.* Figure 1 illustrate essentially linear evaporation kinetics of SiO<sub>2</sub> and AN melts. SEM studies of SiO<sub>2</sub> residues show that while in a short duration runs Ir powder is uniformly distributed in the samples, in a longer runs Ir starts to build up on the surface that lowers the effective evaporating surface and thus evaporation rate. Fig. 1 also show significantly faster evaporation of AN melt compared to that of molten SiO<sub>2</sub>. Since loss of Si from AN melt decreases activity of SiO<sub>2</sub> in the residual melt (and thus evaporation kinetics), only short duration experiments were used to obtain evaporation rates of AN melt.

2) *Evaporation coefficients.* According to thermodynamic calculations, evaporation of SiO<sub>2</sub> and AN melts essentially occur via a loss of SiO<sub>(g)</sub> and O<sub>2(g)</sub>. Therefore, experimentally measured weight loss rates can be used to calculate  $P_{SiO} + P_{O_2}$  above a droplet during evaporation. Figure 2 compares vapor pressures during free evaporation (from a 2.5 mm wire-loop) and equilibrium evaporation (from a cell with 1.0 mm orifice) experiments using vacuum TGA furnace at NASA GRC. The experiments allowed us to determine evaporation coefficients  $\gamma_{Si} = 0.035$  for SiO<sub>2</sub> and  $\gamma_{Si}$

$\gamma_{Si} = 0.11$  for AN melt. Note that  $\gamma_{Si}$  is independent of temperature within the range from 1600° to 1800°C. The value of  $\gamma_{Si} = 0.035$  for  $SiO_2$  agrees with  $\gamma_{Si} = 0.038$ – $0.048$  determined by Hashimoto [5] at 1900°–2100°C and not very different from the values determined for solid  $SiO_2$  ([4] and references therein). Our value of  $\gamma_{Si} = 0.11$  for AN melt is close to  $\gamma_{Si} \sim 0.2$  for molten forsterite at 1890°–2050°C [5] and  $\gamma_{Si} \sim 0.13$  calculated for Type B CAI-like melt evaporated in vacuum at 1800°C [7]. However, strong temperature effect on  $\gamma_{Si}$  ( $\gamma_{Si} \sim 0.10$  at 1700°C, 0.07 at 1600°C, and 0.05 at 1500°C) was reported in [7] while we found no such an effect for both  $SiO_2$  and AN melts within the temperature range studied (Fig. 2).

3) *Silicon isotopic fractionation.* Isotopic composition of silicon in the evaporation residues is presented in the Table. The data show that evaporation of molten  $SiO_2$  does not result (within uncertainties) in any significant or predictable degree of Si isotopic fractionation. This is very different from what is measured in AN melts, evaporated at the same conditions: AN evaporation residues are strongly enriched in heavy isotopes at the levels close to what was reported previously for CAI-like composition melts. We are not aware of isotopic composition measurements in experiments with molten  $SiO_2$ . However, Young et al. [8] have measured oxygen isotopic composition in solid  $SiO_2$  evaporated in vacuum and in low-pressure  $H_2$  gas, and found  $\delta^{18}O$  up to 7–8‰ in highly evaporated (80–90% wt loss) residues but very little fractionation ( $<1\%$ ) in samples that lost  $<30\%$  of the mass.  $\delta^{26}Mg$  up to 30‰ have been measured in [9] but only on a surface layer (a few  $\mu m$ ) of solid forsterite evaporated in vacuum. Lack of isotopic fractionation in molten  $SiO_2$  in our experiments is possibly due to a slow isotopic exchange in very viscous  $SiO_2$  melt.

Si isotopic fractionation factors for AN melt are  $\alpha_{29,28} = 0.9922 \pm 0.0003$  and  $\alpha_{30,28} = 0.9845 \pm 0.0006$  (Fig. 3). The values are close to those reported for molten  $Mg_2SiO_4$  [10], but slightly larger than the values we previously found for melilitic and forsteritic melts (e.g., [3, 7]). Temperature effect on Si isotopic fractionation factor of AN melt should be determined.

**Conclusion:** 1) Comparing free and equilibrium evaporation rates we experimentally determined the evaporation coefficients of  $\gamma_{Si} = 0.035$  for  $SiO_2$  and  $\gamma_{Si} = 0.11$  for AN melts; 2) Free evaporation of molten  $SiO_2$  does not appear to affect the bulk silicon isotopic composition of the evaporating droplets; 3) Evaporation of AN melt result in residues strongly enriched in heavy  $^{29,30}Si$  with isotopic fractionation factors similar to those for molten  $Mg_2SiO_4$ .

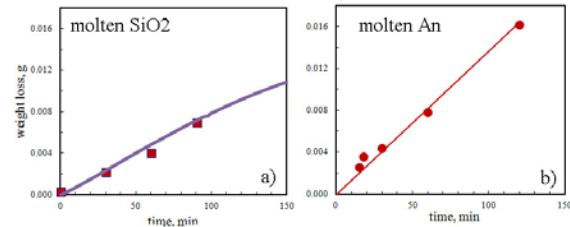


Fig. 1. Free evaporation kinetics of  $SiO_2$  (a) and AN (b) melts at 1800°C in vacuum.

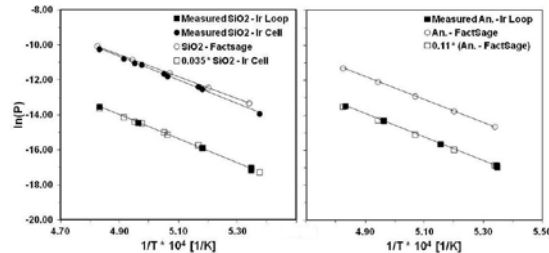


Fig. 2. Vapor pressure above samples during free and equilibrium evaporation of  $SiO_2$  (left) and AN (right) melts as a function of temperature.

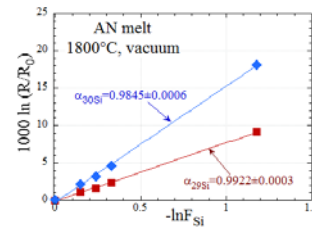


Fig.3.  $^{29}Si$  and  $^{30}Si$  isotopic fractionation factors for AN melt evaporated at 1800°C in vacuum.

Sample	fraction evap.	Composition, wt%			$\delta^{30}Si$	2std	$\delta^{29}Si$	2std
$SiO_2$ start		$SiO_2$	$Al_2O_3$	CaO	-0.07	0.07	-0.04	0.03
$SiO_2$ start repl.					-0.07	0.02	-0.04	0.02
Q1Ir-10	0.01				0.06	0.12	0.03	0.04
Q1Ir-12	0.07				0.05	0.06	0.01	0.03
Q1Ir-13	0.13				0.17	0.02	0.09	0.01
Q1Ir-14	0.23				0.05	0.09	0.00	0.04
Q1Ir-14 repl.	0.23				0.02	0.04	0.01	0.02
Q1Ir-2	0.32				-0.03	0.06	-0.02	0.02
AN1-14	0.00	42.6	36.9	20.5				
AN1-10	0.14	39.0	39.2	21.8	2.12	0.05	1.05	0.04
AN1-12	0.21	36.7	40.4	22.6	3.17	0.05	1.59	0.02
AN1-13	0.28	34.8	41.8	23.4	4.55	0.08	2.27	0.04
AN1-9	0.69	18.6	52.3	29.1	18.21	0.18	9.14	0.09
BHVO-2					-0.34	0.05	-0.18	0.04
BHVO-2					-0.28	0.05	-0.16	0.04
Diatomite					1.17	0.10	0.62	0.02
BCR-2					-0.27	0.10	-0.12	0.04

**References:** [1] Stolper E. and Paque J. M. (1986) *GCA*, 50, 1785–1806. [2] Mendybaev R. A. et al. (2006) *GCA*, 70, 2622–2642. [3] Mendybaev R. A. et al. (2021) *GCA*, 292, 557–576. [4] Jacobson N. et al. (2017) *J. Eur. Ceram. Soc.* 37, 2245–2252. [5] Hashimoto A. (1990) *Nature*, 347, 53–55. [6] Savage P. S. and Moynier F. (2013) *EPSL*, 361, 487–496. [7] Richter F. M. et al. (2007) *GCA*, 71, 5544–5564. [8] Young E. D. (1998) *GCA*, 62, 3109–3116. [9] Wang J. et al. (1999) *GCA*, 63, 953–966. [10] Davis A. M. et al. (1990) *Nature*, 347, 655–658.